

Article

Source Apportionment of PM_{2.5}, PAH and Arsenic Air Pollution in Central Bohemia

Radim Seibert * , Irina Nikolova , Vladimíra Volná , Blanka Krejčí  and Daniel Hladký

Air Quality Department, Czech Hydrometeorology Institute, 708 00 Ostrava, Czech Republic; irina.nikolova@chmi.cz (I.N.); vladimira.volna@chmi.cz (V.V.); blanka.krejci@chmi.cz (B.K.); daniel.hladky@chmi.cz (D.H.)

* Correspondence: radim.seibert@chmi.cz

Abstract: The results of air quality monitoring show significantly increased concentrations of polycyclic aromatic hydrocarbons (PAH) and arsenic in the area located near the town of Kladno in Central Bohemia, Czech Republic. The region of interest is historically associated with coal mines and steelworks. Source apportionment using the method of Positive Matrix Factorization (PMF) at three sites has been used to try to explain the reasons of the increased PM_{2.5}, benzo[*a*]pyrene, and arsenic concentrations in the ambient air. Based on the PMF analysis, nine factors explaining the atmospheric aerosol mass have been identified. The PMF results showed that most of the aerosol mass originated from residential heating (about one third of PM_{2.5}), both primary particles and secondary organic aerosols induced by road traffic (up to approximately 25%), soil and other mineral dust (about 15%), secondary inorganic aerosol ammonium sulfate (up to 16%), ammonium nitrate (up to 14%) and other sulfates (up to 9%). The main source of arsenic and benzo[*a*]pyrene was residential heating, which accounted for two-thirds and 80% of their total mass, respectively. The results have pointed to the most important measures for effective air quality protection in the area of interest: replacing coal fuel and old boilers used for residential heating in order to reduce arsenic and PAH emissions and mitigate sources of secondary particles precursors to decrease PM concentrations.

Keywords: source apportionment; PMF (Positive Matrix Factorization); air pollution; PM_{2.5}; arsenic; heavy metals; benzo[*a*]pyrene; polycyclic aromatic carbohydrates; PAH; heating; coal



Citation: Seibert, R.; Nikolova, I.; Volná, V.; Krejčí, B.; Hladký, D. Source Apportionment of PM_{2.5}, PAH and Arsenic Air Pollution in Central Bohemia. *Environments* **2021**, *8*, 107. <https://doi.org/10.3390/environments8100107>

Academic Editors: Yu-Hsiang Cheng, Elisabete Carolino and Chi-Chi Lin

Received: 14 September 2021

Accepted: 8 October 2021

Published: 13 October 2021

Publisher's Note: MDPI stays neutral with regard to jurisdictional claims in published maps and institutional affiliations.



Copyright: © 2021 by the authors. Licensee MDPI, Basel, Switzerland. This article is an open access article distributed under the terms and conditions of the Creative Commons Attribution (CC BY) license (<https://creativecommons.org/licenses/by/4.0/>).

1. Introduction

The measurement results from the National Air Quality Monitoring Network of the Czech Republic and from the recently performed projects of the Czech Hydrometeorological Institute show significantly increased concentrations of polycyclic aromatic hydrocarbons (PAHs) and arsenic in the central part of the Czech Republic near the city of Kladno. The affected region is located within the connecting lines between the cities of Kladno, Louny, Rakovník, Žatec, and Beroun, with a total area of approximately 850 km² (Figure 1a).

The area of interest is characterized by the occurrence of localities with high concentrations of benzo[*a*]pyrene and arsenic. The highest concentrations of benzo[*a*]pyrene and arsenic in the area are observed in Kladno and its surrounding areas, as well as in small settlements with predominant individual heating with solid fuels [1]. According to [2–5], the average annual concentrations of benzo[*a*]pyrene in some localities in the area are up to more than twice their annual limit value [6]. Although the average annual concentrations of As in the area of interest do not exceed the annual limit, high daily values of As are measured in the winter, and the average concentrations of winter months are significantly higher than the value of the annual limit [2–5]. The above information based on stationary stations with year-round measurement is complemented by campaign project measurements [7]. These campaign measurements focus only on the part of the year. Therefore, the annual average cannot be calculated from the measured data. However, the measured daily concentrations of benzo[*a*]pyrene and arsenic in some localities of the area of interest reach

values several-fold higher than their annual limits [8,9]. We assume the data regarding the spatial distribution of benzo[*a*]pyrene and arsenic concentrations [1,7,10,11] are undervalued due to the insufficiently dense network of stations with heavy metal measurements.

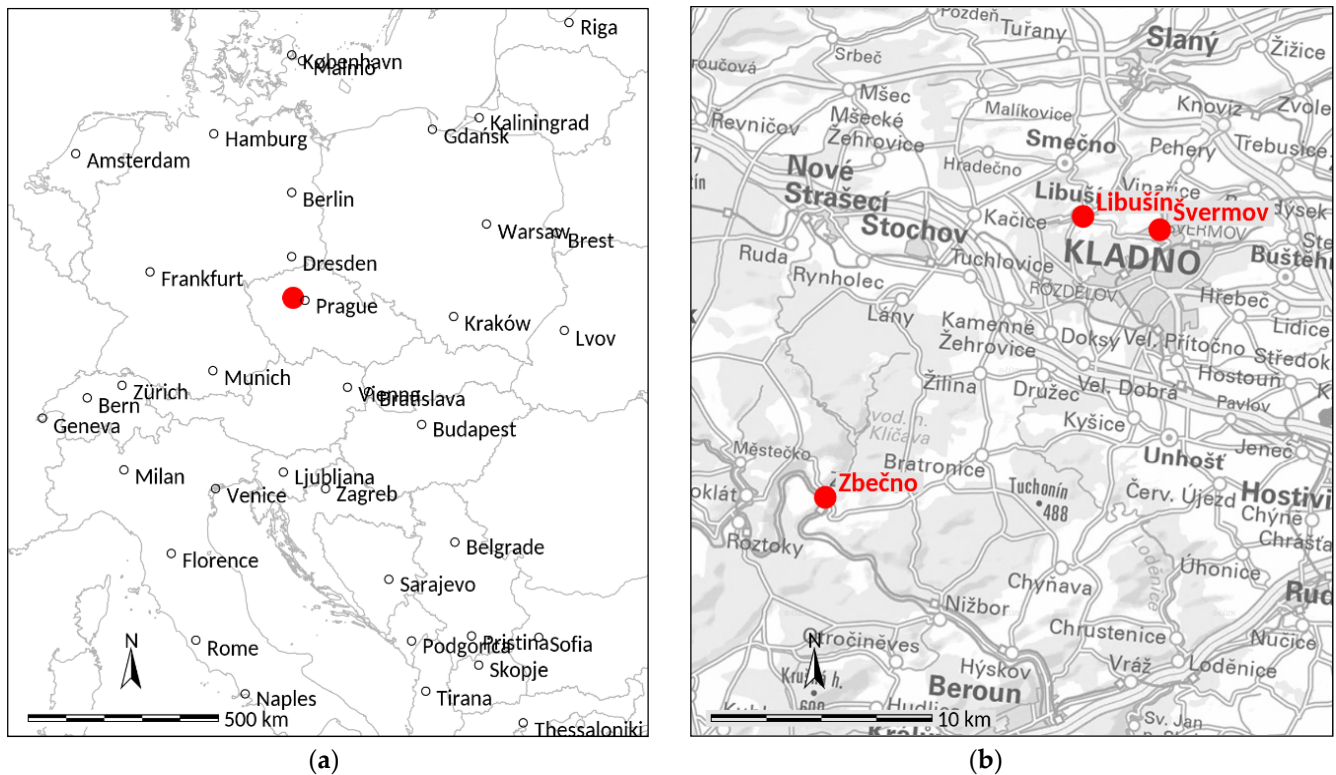


Figure 1. The location of the area of interest: (a) Position within Central Europe; (b) Sampling site locations. Topography base: (a) Made with Natural Earth. Free vector and raster map data at [naturalearthdata.com](https://www.naturalearthdata.com); (b) ČÚZK, State Administration of Land Surveying and Cadastre.

To find out reasons for the worse air pollution level, a source apportionment based on air quality measurement, PMF modelling and model interpretation, has been carried out within a recent research project [12]. Three sites have been selected for the source apportionment: Švermov, which represents the northern part of Kladno; the small town of Libušín, located at a distance of approximately 3.5 km west from Švermov; and the small village of Zbečno located approximately 17 km and 19 km to the southwest of Libušín and Švermov, respectively.

There are significant differences among the Libušín, Švermov, and Zbečno monitoring sites regarding land use, local pollution sources, and terrain. Švermov is the most urbanized of the three monitoring sites. Kladno is the administrative center with abundant high-rise buildings, whereas Švermov, due to its mining history, consists of low-rise houses of relatively small size. Recently, due to the previous radical reduction in heavy industry activities in Kladno and its neighboring towns, road traffic can be assumed to be the most important anthropogenic local air pollution source here. The annual average of daily traffic intensity at the nearest road (about 50 m from the Švermov monitoring site) was about 10,000 vehicles per 24 h [13]. Soil and crustal particles suspended by the wind from paved surfaces are also expected to be significant source of air pollution. Previous research results [8,9] show that traditional strong dependency of residential heating on coal fuel is a common feature in the entire Kladno region. This fundamentally influences concentrations of air pollutants and their seasonal trends, including PAHs and heavy metals. Švermov can be classified as an urban background site. It is located in a small local terrain depression. The terrain in the vicinity is wavy, with elevation differences of about 100 m.

Libušín is somewhat less urbanized than Švermov. It can be considered a small town or a larger village. The monitoring station was located right in its center. The settlement is predominantly composed of low-rise buildings. Residential heating and moderate road traffic play the most important role at this site, as they are the only significant local anthropogenic air pollution sources here. The annual average of daily traffic intensity at the nearest road is approximately 3000 vehicles per 24 h (estimation based on the traffic counting in other towns of similar size in the Kladno region). The crustal material (resuspended dust) is less significant in Libušín. The terrain characteristics in Libušín are similar to those in Švermov. Libušín can be considered an urban background site.

Zbečno is a rural monitoring site located in the centre of a small village. As it is situated at the bottom of a river valley with steep slopes of a height of about 200 m, significant variations of local wind speed, direction, and limited air mixing conditions are assumed here compared to those nearby. In contrast to Švermov and Libušín, there is no natural gas distribution network in Zbečno. Residential heating demands are covered only by the local solid-fuel boilers installed in the family houses. Activity of other local air pollution sources in Zbečno is very limited. The average daily intensity of road traffic here is only about 900 vehicles per 24 h (the nearest road was located approximately 20 m from the monitoring site) [13]. There are no known industrial activities with significant emissions here. The only exception is a spilite quarry in the neighboring village of Sýkořice.

2. Materials and Methods

2.1. Sample Collection

The samples were collected at the sampling sites of Libušín, Švermov, and Zbečno. Different sources influencing the air quality in different parts of the surveyed area were thus taken into account. Subsequently, measurements from the all monitoring sites were merged for the PMF model. This approach allowed us to obtain a larger dataset and more robust and more representative PMF results than could be provided by modeling the individual locations. Samples collected at different sites have already been used in many other PMF source apportionment studies, and the approach has proven to increase the statistical significance of the analysis, although it assumes that chemical profiles of sources do not vary at the different sites [14] (pp. 134–136). The measurement consisted of summer and winter parts. The summer sampling was carried out from 28 June 2019 6:00 a.m. to 28 July 2019 6:00 p.m. The winter sampling was carried out from 14 November 2019 6:00 a.m. to 15 December 2019 6:00 p.m. All times in this paper are given in coordinated universal time (UTC). The number of samples collected and subsequently lab processed was 61 and 63 at each site in the summer and winter, respectively. A total of 372 samples were used for receptor modelling. This number of samples is sufficient for reliable source apportionment based on the PMF model, as it is in accordance with its official user guide [15] (PMF is often used on speciated PM_{2.5} datasets with a size above 100 samples.)

The automatic sequential samplers (Sven Leckel SEQ, Ingenieurbüro GmbH, Berlin, Germany) were used for the atmospheric aerosol sampling at all sites. The samples of PAHs and hopanes were collected in 47 mm quartz fiber filters. The same quartz fiber filters were also used for anhydrosugars and organic and elemental carbon (OC/EC) analysis. For the ED XRF and gravimetric PM_{2.5} mass analysis, samplings using PTFE and cellulose nitrate filters of the same size were performed, respectively.

All the dust aerosol samples were collected continuously for 12 h. During the collection of all the samples, sampling flows and collection heads (DIGITEL Low Volume pre-separators) were used, ensuring representative sampling of the PM_{2.5} fraction. The measurement of wind speed and direction and gaseous pollutants was carried out at all the sites by automatic analyzers placed inside mobile air quality monitoring vehicles.

2.2. Laboratory Analyses

The lab analyses were performed at the Czech Hydrometeorological Institute, with an exception of the determination of the Na^+ , K^+ , Ca^{2+} , and Mg^{2+} concentrations, which was done in the laboratories of the ALS Czech Republic, s.r.o. company (Prague, Czech Republic). In all the collected aerosol samples, the same species were analyzed using the following methods to determine ambient air concentrations:

- gravimetric analysis: $\text{PM}_{2.5}$ mass
- thermo-optical transmission: organic and elemental carbon (OC/EC)
- spectrometric analysis: ammonia (NH_4^+)
- optical emission spectrometry with inductively coupled plasma (ICP-OES): Na^+ , K^+ , Ca^{2+} , Mg^{2+}
- ion chromatography with conductivity detection (IC-CD): sulfates and nitrates (SO_4^{2-} , NO_3^-)
- gas chromatography with mass detection (GC-MS). The internal standard method is used to determine the concentrations of analytes:
 - PAH (benzo[*a*]anthracene (BaA), benzo[*a*]pyrene (BaP), benzo[*b*]fluoranthene (BbF), benzo[*e*]pyrene (BeP), benzo[*ghi*]perylene (BghiPRL), benzo[*j*]fluoranthene (BjF), benzo[*k*]fluoranthene (BkF), coronene (COR), chrysene (CRY), fluoranthene (FLU), indeno [1,2,3-*cd*]pyrene (I123cdP), picene (PIC), perylene (PRL), pyrene (PYR), retene (RET)),
 - hopanes (17 α (H)-22,29,30-trisnorhopane, 17 α (H),21 β (H)-30-norhopane, 17 α (H),21 β (H)-hopane, 17 β (H),21 α (H)-hopane, 22S-17 α (H),21 β (H)-homohopane, 22R-17 α (H),21 β (H)-homohopane),
 - steranes ($\alpha\alpha\alpha$ 20S-cholestane, $\alpha\beta\beta$ (20R)-cholestane, $\alpha\alpha\alpha$ 20R-cholestane, $\alpha\beta\beta$ 20R 24S-methylcholestane, $\alpha\beta\beta$ 20R 24R-ethylcholestane, $\alpha\alpha\alpha$ 20R 24R-ethylcholestane)
- high-performance anion-exchange chromatography with pulsed amperometric detection (IC HPAE-PAD): levoglucosan, mannosan, galactosan
- energy dispersive X-ray fluorescence (ED XRF): Na, Mg, Al, Si, S, K, Ca, Ti, V, Cr, Mn, Fe, Ni, Cu, Zn, As, Se, Cd, Sb, Ba, Pb, Cl
- continuous analyzer measurement:
 - UV-fluorescence (Teledyne Advanced Pollution Instrumentation T100): SO_2
 - chemiluminescence (Teledyne Advanced Pollution Instrumentation T200): nitrogen oxides (NO , NO_2 , NO_x)
 - optoelectronic method (FIDAS 200): $\text{PM}_{2.5}$

3. Results

3.1. Wind Speed and Direction at the Sampling Sites

The following wind roses (Figure 2) document the situation at the sampling sites during the summer and winter sampling periods.

The prevailing wind direction in Libušín and Švermov was almost the same. Generally, the most frequent was the west direction here. In the winter, wind flow from eastern directions was more frequent compared to the summer. At the Libušín site, east and northeast directions were the most frequent ones in the winter. In the winter, average wind speed was significantly higher at both of the mentioned sites (approximately from 0.5 to 0.6 $\text{m}\cdot\text{s}^{-1}$ in the summer and 0.9 to 1.3 $\text{m}\cdot\text{s}^{-1}$ in the winter). In contrast, the wind measurement in Zbečno shows the prevailing directions in accordance with the river canyon course (northwest and south are the most frequent). A lower average wind speed and its negligible difference between seasons was observed here (approximately 0.5 and 0.4 $\text{m}\cdot\text{s}^{-1}$ in the summer and winter). The lower wind speed and more frequent calm in Zbečno (1.3 and 5.7% in the summer and winter, respectively) compared to Libušín and Švermov (0.5–0.7% in the summer and 0.7% in the winter) prove the limited local air mixing conditions.

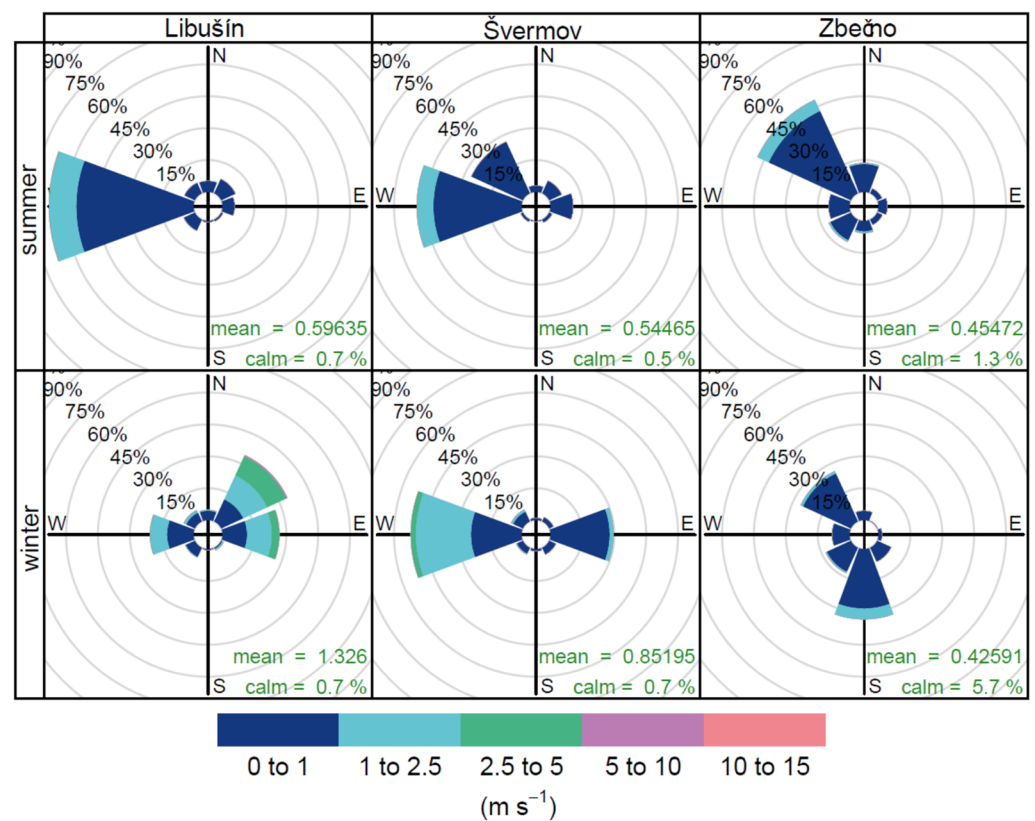


Figure 2. Seasonal wind roses representing the sampling periods.

3.2. Measured Concentrations

The summary Table 1 lists the minimum, maximum, median, and percentages of below detection limit and missing observations of species. (Values below the detection limit were replaced by half of the detection limit for statistical processing.)

All the measured data used for the PMF model is a supplementary material of the article (Table S1: Measured concentrations and uncertainties). The measured data show higher concentrations of organic and elemental carbon, PAHs, some metals, potassium, sulfur, nitrates, ammonium ion, and anhydrosacharides during the winter sampling campaign. On the other hand, most of the typical crustal species such as Ba, Mg, Al, Ca, Ti show higher concentrations in the summer. Figure 3 illustrates the main components of the PM_{2.5} mass concentrations and their differences among the individual monitoring sites. As carbon mass present in levoglucosan is part of organic carbon, only hydrogen and oxygen are counted in the levoglucosan amount in Figure 3 (about 55.5%).

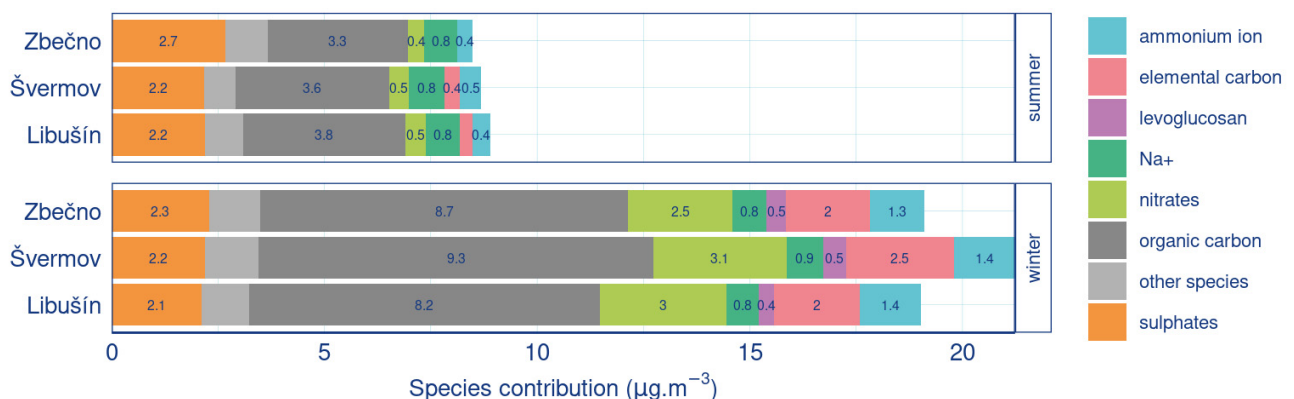


Figure 3. Mass composition of PM_{2.5}.

Table 1. Species quantified in this study (summary of all three sampling sites). BDL: Below detection limit; N/A: no data available.

Species	Summer					Winter				
	Min (ng.m ⁻³)	Max (ng.m ⁻³)	Median (ng.m ⁻³)	Percent BDL	Percent Missing	Min (ng.m ⁻³)	Max (ng.m ⁻³)	Median (ng.m ⁻³)	Percent BDL	Percent Missing
PM _{2.5}	5.2 × 10 ³	2.8 × 10 ⁴	1.2 × 10 ⁴	0%	0%	1.6 × 10 ³	7.8 × 10 ⁴	2.1 × 10 ⁴	0%	0%
OC	1.6 × 10 ³	8.3 × 10 ³	3.4 × 10 ³	0%	13%	1.7 × 10 ³	3.7 × 10 ⁴	6.8 × 10 ³	0%	1%
EC	5.7 × 10 ¹	8.2 × 10 ²	2.7 × 10 ²	0%	13%	2.5 × 10 ²	1.1 × 10 ⁴	1.8 × 10 ³	0%	1%
OC1	5.2 × 10 ²	2.8 × 10 ³	1.1 × 10 ³	0%	13%	5.6 × 10 ²	1.7 × 10 ⁴	2.0 × 10 ³	0%	1%
OC2	2.1 × 10 ²	1.7 × 10 ³	5.9 × 10 ²	0%	13%	2.4 × 10 ²	5.3 × 10 ³	8.7 × 10 ²	0%	1%
OC3	2.5 × 10 ²	2.2 × 10 ³	6.7 × 10 ²	0%	13%	2.9 × 10 ²	3.6 × 10 ³	9.8 × 10 ²	0%	1%
OC4	2.2 × 10 ²	8.3 × 10 ²	4.6 × 10 ²	0%	13%	2.0 × 10 ²	1.7 × 10 ³	7.6 × 10 ²	0%	1%
EC1	1.0 × 10 ²	1.3 × 10 ³	3.2 × 10 ²	0%	13%	2.4 × 10 ²	8.4 × 10 ³	2.0 × 10 ³	0%	1%
EC2	6.7 × 10 ¹	7.3 × 10 ²	2.1 × 10 ²	0%	13%	2.1 × 10 ²	7.7 × 10 ³	1.6 × 10 ³	0%	1%
EC3	6.2 × 10 ¹	6.3 × 10 ²	2.2 × 10 ²	0%	13%	2.1 × 10 ¹	1.1 × 10 ³	3.2 × 10 ²	0%	1%
EC4	8.2 × 10 ⁰	1.5 × 10 ²	2.8 × 10 ¹	0%	13%	−1.3 × 10 ¹	4.0 × 10 ²	7.7 × 10 ¹	0%	1%
Ca ²⁺	1.1 × 10 ²	3.1 × 10 ²	1.7 × 10 ²	0%	0%	6.2 × 10 ¹	6.0 × 10 ²	1.5 × 10 ²	0%	0%
K ⁺	1.5 × 10 ¹	8.3 × 10 ²	1.1 × 10 ²	0%	0%	3.9 × 10 ¹	6.3 × 10 ²	1.7 × 10 ²	0%	0%
Mg ²⁺	2.0 × 10 ¹	1.3 × 10 ²	4.7 × 10 ¹	0%	0%	2.4 × 10 ¹	1.3 × 10 ²	5.0 × 10 ¹	0%	0%
Na ⁺	1.3 × 10 ²	1.4 × 10 ³	8.4 × 10 ²	0%	0%	5.0 × 10 ²	1.2 × 10 ³	8.0 × 10 ²	0%	0%
NH ₄ ⁺	8.1 × 10 ⁻¹	1.5 × 10 ³	4.0 × 10 ²	0%	0%	4.9 × 10 ¹	4.0 × 10 ³	1.3 × 10 ³	0%	0%
NO ₃ ⁻	1.6 × 10 ²	1.2 × 10 ³	4.0 × 10 ²	0%	0%	3.3 × 10 ²	1.1 × 10 ⁴	2.5 × 10 ³	0%	0%
SO ₄ ²⁻	7.0 × 10 ²	6.3 × 10 ³	2.1 × 10 ³	0%	0%	5.2 × 10 ²	7.1 × 10 ³	1.9 × 10 ³	0%	0%
Al	9.7 × 10 ¹	4.5 × 10 ²	1.8 × 10 ²	63%	0%	3.2 × 10 ¹	3.7 × 10 ²	4.6 × 10 ¹	0%	0%
As	2.1 × 10 ⁰	8.9 × 10 ⁰	2.1 × 10 ⁰	24%	0%	9.7 × 10 ⁻¹	1.3 × 10 ²	7.6 × 10 ⁰	0%	0%
Ba	4.2 × 10 ⁻¹	1.2 × 10 ¹	2.6 × 10 ⁰	3%	0%	1.5 × 10 ⁻¹	6.6 × 10 ⁰	1.2 × 10 ⁰	0%	0%
Ca	8.4 × 10 ⁰	4.4 × 10 ²	8.4 × 10 ¹	75%	0%	4.5 × 10 ⁰	6.3 × 10 ²	3.4 × 10 ¹	0%	0%
Cl	N/A	N/A	N/A	0%	100%	3.9 × 10 ¹	1.6 × 10 ³	1.9 × 10 ²	0%	0%
Cr	6.7 × 10 ⁰	8.3 × 10 ⁰	7.5 × 10 ⁰	75%	0%	1.3 × 10 ⁻¹	4.4 × 10 ⁰	5.3 × 10 ⁻¹	0%	0%
Cu	4.4 × 10 ⁻¹	8.7 × 10 ⁰	1.5 × 10 ⁰	31%	0%	8.7 × 10 ⁻¹	1.2 × 10 ¹	3.4 × 10 ⁰	0%	0%
Fe	1.6 × 10 ¹	2.7 × 10 ²	9.6 × 10 ¹	92%	0%	6.0 × 10 ⁰	6.5 × 10 ²	5.5 × 10 ¹	0%	0%
K	8.9 × 10 ⁰	3.7 × 10 ²	6.3 × 10 ¹	76%	0%	3.2 × 10 ¹	6.0 × 10 ²	2.0 × 10 ²	0%	0%
Mg	1.7 × 10 ¹	1.1 × 10 ²	4.6 × 10 ¹	23%	0%	7.7 × 10 ⁰	2.9 × 10 ²	3.9 × 10 ¹	0%	0%
Mn	5.5 × 10 ⁻¹	6.3 × 10 ⁰	2.1 × 10 ⁰	10%	0%	1.5 × 10 ⁻¹	1.2 × 10 ¹	1.8 × 10 ⁰	0%	0%
Na	4.9 × 10 ⁰	1.1 × 10 ²	2.9 × 10 ¹	11%	0%	1.6 × 10 ¹	2.0 × 10 ²	5.8 × 10 ¹	0%	0%
Ni	4.1 × 10 ⁻¹	1.1 × 10 ⁰	4.1 × 10 ⁻¹	5%	0%	3.1 × 10 ⁻²	1.6 × 10 ⁰	2.1 × 10 ⁻¹	0%	0%
Pb	6.9 × 10 ⁻¹	2.0 × 10 ¹	1.8 × 10 ⁰	24%	0%	1.9 × 10 ⁰	4.6 × 10 ¹	1.2 × 10 ¹	0%	1%
S	1.4 × 10 ²	1.2 × 10 ³	4.5 × 10 ²	14%	0%	1.8 × 10 ²	2.2 × 10 ³	8.3 × 10 ²	0%	0%

Table 1. Cont.

Species	Summer					Winter				
	Min (ng.m ⁻³)	Max (ng.m ⁻³)	Median (ng.m ⁻³)	Percent BDL	Percent Missing	Min (ng.m ⁻³)	Max (ng.m ⁻³)	Median (ng.m ⁻³)	Percent BDL	Percent Missing
Sb	1.1×10^{-1}	2.9×10^0	6.0×10^{-1}	24%	0%	1.9×10^1	1.3×10^2	2.7×10^1	0%	0%
Se	3.0×10^{-1}	1.9×10^0	8.8×10^{-1}	8%	0%	7.8×10^{-2}	3.1×10^0	7.8×10^{-1}	0%	0%
Ti	8.2×10^{-1}	3.0×10^1	8.0×10^0	10%	0%	9.4×10^{-2}	5.4×10^1	2.6×10^0	0%	0%
V	2.8×10^{-1}	1.8×10^0	2.8×10^{-1}	0%	0%	2.7×10^{-2}	2.2×10^0	2.6×10^{-1}	0%	0%
Zn	1.5×10^0	2.3×10^1	6.1×10^0	24%	0%	4.8×10^0	2.0×10^2	2.3×10^1	0%	0%
BaA	1.5×10^{-2}	3.5×10^{-1}	1.5×10^{-2}	74%	0%	2.4×10^{-1}	4.3×10^1	3.7×10^0	0%	0%
BaP	1.5×10^{-2}	3.9×10^{-1}	1.5×10^{-2}	64%	0%	1.8×10^{-1}	2.4×10^1	2.4×10^0	0%	0%
BbF	1.5×10^{-2}	4.4×10^{-1}	4.0×10^{-2}	36%	0%	3.7×10^{-1}	1.8×10^1	2.8×10^0	0%	0%
BeP	1.5×10^{-2}	3.1×10^{-1}	1.5×10^{-2}	66%	0%	2.1×10^{-1}	1.0×10^1	1.5×10^0	0%	0%
BghiPRL	1.5×10^{-2}	3.6×10^{-1}	5.0×10^{-2}	33%	0%	4.0×10^{-2}	1.5×10^1	2.0×10^0	0%	0%
BjF	1.5×10^{-2}	2.7×10^{-1}	1.5×10^{-2}	81%	0%	2.0×10^{-1}	1.2×10^1	1.6×10^0	0%	0%
BkF	1.5×10^{-2}	2.1×10^{-1}	1.5×10^{-2}	76%	0%	1.8×10^{-1}	1.1×10^1	1.4×10^0	0%	0%
Coronene	2.0×10^{-2}	1.4×10^{-1}	2.0×10^{-2}	93%	0%	5.0×10^{-2}	3.6×10^0	4.8×10^{-1}	0%	0%
Chrysene	1.5×10^{-2}	3.0×10^{-1}	1.5×10^{-2}	59%	0%	2.6×10^{-1}	3.1×10^1	3.5×10^0	0%	0%
Fluoranthene	4.0×10^{-2}	1.3×10^0	4.0×10^{-2}	57%	0%	4.1×10^{-1}	3.7×10^1	3.5×10^0	0%	0%
I123cdP	1.5×10^{-2}	4.3×10^{-1}	5.0×10^{-2}	33%	0%	3.2×10^{-1}	2.2×10^1	2.7×10^0	0%	0%
Perylene	1.5×10^{-2}	8.0×10^{-2}	1.5×10^{-2}	99%	0%	5.0×10^{-2}	4.4×10^0	5.0×10^{-1}	0%	0%
Picene	2.0×10^{-2}	5.0×10^{-2}	2.0×10^{-2}	97%	0%	3.0×10^{-2}	5.0×10^0	5.7×10^{-1}	0%	0%
Pyrene	3.0×10^{-2}	5.0×10^{-1}	3.0×10^{-2}	74%	0%	3.6×10^{-1}	3.7×10^1	3.6×10^0	0%	0%
Retene	3.0×10^{-2}	1.1×10^{-1}	3.0×10^{-2}	98%	0%	1.9×10^{-1}	3.0×10^1	1.6×10^0	0%	0%
17 α (H),21 β (H)-22R-Homohopane	3.5×10^{-2}	2.2×10^{-1}	3.5×10^{-2}	14%	0%	1.4×10^{-1}	1.5×10^1	1.8×10^0	0%	0%
17 α (H),21 β (H)-22S-Homohopane	3.5×10^{-2}	2.7×10^{-1}	3.5×10^{-2}	22%	0%	3.5×10^{-2}	2.0×10^0	2.8×10^{-1}	0%	0%
17 α (H),21 β (H)-30-Norhopane	5.5×10^{-2}	3.2×10^{-1}	1.1×10^{-1}	75%	0%	1.0×10^{-1}	5.3×10^0	8.1×10^{-1}	0%	0%
17 α (H),21 β (H)-Hopane	7.0×10^{-2}	5.0×10^{-1}	1.4×10^{-1}	68%	0%	5.5×10^{-2}	4.3×10^0	6.5×10^{-1}	0%	0%
17 α (H)-22,29,30-Trisnorhopane	3.5×10^{-2}	1.3×10^{-1}	3.5×10^{-2}	19%	0%	7.0×10^{-2}	4.3×10^0	6.5×10^{-1}	0%	0%
17 β (H),21 α (H)-Hopane	3.5×10^{-2}	9.0×10^{-2}	3.5×10^{-2}	17%	0%	8.0×10^{-2}	4.0×10^0	5.9×10^{-1}	0%	0%
$\alpha\alpha\alpha$ 20R-Cholestane	3.5×10^{-2}	7.1×10^{-1}	3.5×10^{-2}	69%	0%	3.5×10^{-2}	1.7×10^{-1}	3.5×10^{-2}	7%	0%
$\alpha\alpha\alpha$ 20R 24R-Ethylcholestane	3.5×10^{-2}	1.7×10^{-1}	3.5×10^{-2}	55%	0%	3.5×10^{-2}	1.9×10^0	2.2×10^{-1}	75%	0%
$\alpha\alpha\alpha$ 20S Cholestane	3.5×10^{-2}	3.5×10^{-2}	3.5×10^{-2}	76%	0%	3.5×10^{-2}	1.3×10^{-1}	3.5×10^{-2}	95%	0%
$\alpha\beta\beta$ 20R Cholestane	3.5×10^{-2}	1.3×10^{-1}	3.5×10^{-2}	61%	0%	3.5×10^{-2}	1.3×10^{-1}	3.5×10^{-2}	94%	0%
$\alpha\beta\beta$ 20R24R Ethylcholestane	3.5×10^{-2}	1.3×10^{-1}	3.5×10^{-2}	67%	0%	3.5×10^{-2}	2.1×10^{-1}	3.5×10^{-2}	92%	0%

Table 1. Cont.

Species	Summer					Winter				
	Min (ng.m ⁻³)	Max (ng.m ⁻³)	Median (ng.m ⁻³)	Percent BDL	Percent Missing	Min (ng.m ⁻³)	Max (ng.m ⁻³)	Median (ng.m ⁻³)	Percent BDL	Percent Missing
$\alpha\beta\beta$ 20R24S Methylcholestane	3.5×10^{-2}	1.8×10^{-1}	3.5×10^{-2}	58%	0%	3.5×10^{-2}	2.1×10^{-1}	3.5×10^{-2}	77%	0%
Levoglucozan	5.1×10^{-1}	3.3×10^2	1.4×10^1	44%	0%	8.1×10^0	5.1×10^3	5.5×10^2	1%	1%
Mannosan	1.8×10^0	8.4×10^1	3.5×10^0	84%	0%	3.5×10^0	8.9×10^2	1.1×10^2	5%	1%
Galactosan	3.5×10^0	3.0×10^1	3.5×10^0	96%	0%	3.5×10^0	2.5×10^2	3.6×10^1	10%	1%
CO	1.3×10^2	4.9×10^2	2.6×10^2	0%	0%	1.8×10^2	1.2×10^3	4.4×10^2	0%	0%
NO	5.0×10^{-1}	3.8×10^0	8.8×10^{-1}	29%	0%	5.0×10^{-1}	4.8×10^1	4.6×10^0	2%	0%
NO ₂	2.8×10^0	1.8×10^1	7.2×10^0	0%	0%	5.4×10^0	4.5×10^1	1.5×10^1	0%	0%
NO _x	3.5×10^0	2.1×10^1	8.8×10^0	0%	0%	6.7×10^0	1.2×10^2	2.3×10^1	0%	0%
SO ₂	1.3×10^0	6.2×10^0	1.8×10^0	35%	0%	2.1×10^0	2.6×10^1	6.8×10^0	0%	0%

Similarly to Figure 3, Table 2 proves the relatively small differences between PM_{2.5}, benzo[*a*]pyrene, and arsenic concentrations among the monitoring sites. In contrast, strong seasonal variation of their concentrations has been observed, especially in the case of benzo[*a*]pyrene (differences of two orders of magnitude). The majority of the species showed nearly lognormal distribution. Based on the comparison of the mean and median values, Table 2 highlights the significant influence of outliers in Zbečno on the average arsenic and benzo[*a*]pyrene concentrations in the winter.

Table 2. Mean and median concentrations of selected species. BDL: Below the detection limit.

Species	Summer					
	Libušín		Švermov		Zbečno	
	Mean (ng·m ⁻³)	Median (ng·m ⁻³)	Mean (ng·m ⁻³)	Median (ng·m ⁻³)	Mean (ng·m ⁻³)	Median (ng·m ⁻³)
PM _{2.5}	11.4 × 10 ³	11.6 × 10 ³	12.4 × 10 ³	12.1 × 10 ³	11.9 × 10 ³	11.7 × 10 ³
Benzo[<i>a</i>]pyrene	2.2 × 10 ⁻²	BDL	3.2 × 10 ⁻²	BDL	4.1 × 10 ⁻²	4.0 × 10 ⁻²
As	2.3 × 10 ⁰	BDL	BDL	BDL	BDL	BDL
Species	Winter					
	Libušín		Švermov		Zbečno	
	Mean (ng·m ⁻³)	Median (ng·m ⁻³)	Mean (ng·m ⁻³)	Median (ng·m ⁻³)	Mean (ng·m ⁻³)	Median (ng·m ⁻³)
PM _{2.5}	22.3 × 10 ³	21.4 × 10 ³	25.4 × 10 ³	22.3 × 10 ³	22.8 × 10 ³	19.6 × 10 ³
Benzo[<i>a</i>]pyrene	3.7 × 10 ⁰	2.5 × 10 ⁰	4.8 × 10 ⁰	3.2 × 10 ⁰	3.0 × 10 ⁰	1.8 × 10 ⁰
As	8.0 × 10 ⁰	7.5 × 10 ⁰	7.7 × 10 ⁰	6.9 × 10 ⁰	1.5 × 10 ¹	8.0 × 10 ⁰

3.3. Positive Matrix Factorization (PMF) Model Results

The PMF model 5.0 was used in accordance with the U.S. EPA Positive Matrix Factorization, Fundamentals and User Guide [15]. The species were categorized based on the signal/noise ratio. A total of 45 species were used in PMF, out of which 37 were STRONG and 8 WEAK. The complete species set used for PMF is provided in the chemical profiles graph in Appendix A. Missing values were replaced with a median by the PMF software. Associated uncertainties were replaced with the values of four times the species-specific median. One-half of the detection limit was assigned to the values below the detection limit, and their uncertainty was replaced by the value of 5/6 of the detection limit.

The concentrations and uncertainties of gaseous species, which do not contribute to the total PM_{2.5} mass, were divided by 1000 to make their effect on the mass of the identified factors negligible. The same approach was used for individual thermal-resolved OC/EC fractions. Their concentrations and uncertainties were reduced by three orders of magnitude to prevent significant overestimation of the OC/EC mass.

Model runs with different parameters were carried out to find an optimal, physically meaningful number of PMF factors. For the dataset without thermal resolved OC/EC fractions, eight clearly interpretable factors were found. In the end, the addition of OC/EC fractions to the dataset allowed us to raise the number of identified factors to nine. For the base solution with the nine factors, 50 runs with an extra model uncertainty of 12% were performed. The Q/Qexp ratio of the best base run solution was 0.98. A regression analysis of the modelled and measured concentrations of PM_{2.5}, benzo[*a*]pyrene, and arsenic (key pollutants in the area of interest) has shown the R² being 0.96, 0.93, and 0.43, respectively. Significantly lower correlation between the modelled and measured arsenic concentrations than in the case of other pollutants is discussed in Chapter 4. The base run solution was slightly rotated (Fpeak = −0,5) to reach 100% accordance with the bootstrap and base run factors and no unmapped factors (20 bootstrap runs were performed). The Q/Qexp ratio of the rotated solution was 1.00.

3.4. Identified PMF Factors

Identified factors and their contribution to the PM_{2.5} mass grouped by season are shown in Figure 4.

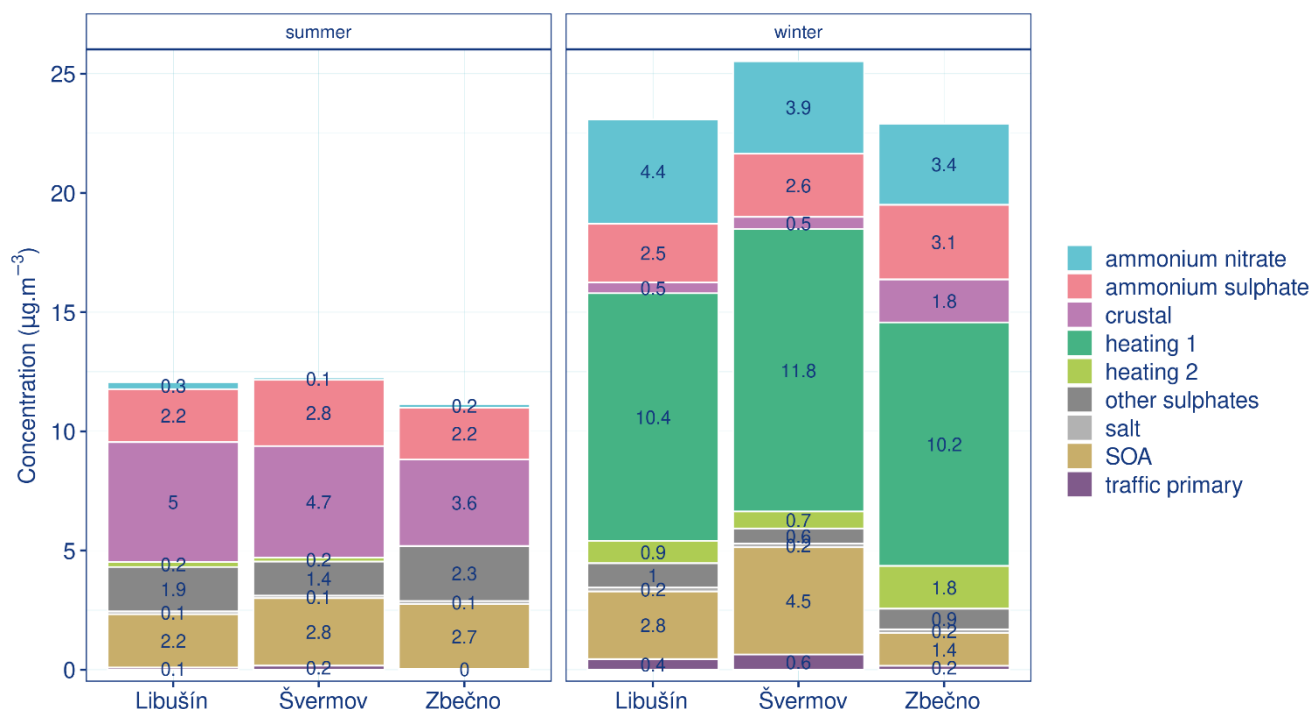


Figure 4. Factor absolute contribution to the PM_{2.5} mass grouped by season and monitoring sites.

Based on the factor chemical profiles (Appendix A) and time series (Appendix B), the main characteristics of the identified factors can be summarized as follows:

The ammonium nitrate factor profile contains a dominant percentage of nitrate and ammonium ions, which are accompanied by a smaller ratio of nitrogen oxides and zinc. The factor has no daily variation but shows a strong seasonal variation. Its concentration is negligible in the summer and the second highest in the winter.

The ammonium sulfate factor is distinguished by its dominant ratio of sulfate and ammonium ions. Daily variation is low and apparent only in the summer. Seasonal variation is insignificant, with only slightly higher concentrations in the winter.

The crustal factor can easily be recognized on the basis of a high percentage of typical crustal elements (Ba, Ca, Fe, Mn, Ti). Daily and seasonal variation is strong with higher concentrations during the daytime and the summer.

The heating 1 factor has a dominant ratio of polycyclic aromatic hydrocarbons (PAH), anhydrosaccharides, and elemental carbon (EC), with a significant percentage of organic carbon (OC). The majority of thermal-resolved fractions of both organic and elemental carbon are of low-temperature (decreasing percentage from EC1 to EC4 and OC1 to OC4). The factor profile shows also accessory elements (K, Pb, Zn, Cl). The factor has apparent daily variation and the highest seasonal variation of all the identified factors.

The heating 2 factor was separated from the heating 1 factor. It has a similar daily and seasonal variation to the heating 1 factor. Heating 1 and heating 2 had been combined into just one factor in preliminary model solutions with a lower number of PMF factors. Increasing the number of model factors led to a division of residential heating factors between the two individual factors. Such a factor separation significantly decreased model-scaled residua of arsenic and is meaningful due to the different characteristics of residential heating at the monitoring sites. The time series of the factor contribution (see Appendix B) shows significantly higher levels at the Zbečno site, which is of rural character and without a natural gas distribution network. Thus, only solid fuels (coal and biomass) are used for

heating in Zbečno. In contrast, Libušín and Švermov are suburban sites with probable different behavior of inhabitants regarding heating practices and a higher share of natural gas in the fuel mix.

The other sulfates factor contains water-soluble ions and the sulfate ion that indicates aged pollution from non-local sources. The factor chemical profile also includes a high percentage of selenium and vanadium. The factor shows no daily variation, but its seasonal variation is significant. A higher contribution of the factor to the PM_{2.5} mass was found in the summer.

The salt factor profile is composed of mainly Na, Mg, Cl, Na⁺, and Mg²⁺. Considering the effect of chemical transformations during atmospheric aerosol transport, the sodium and magnesium ratio in the factor profile (3.9 ng·m⁻³/0.5 ng·m⁻³) is similar to the ratio in sea water. (The Mg concentration in sea water is about five times lower than that of Ca [16].) The salt factor has no apparent daily variation. Its winter concentrations are slightly higher than those in the summer.

The secondary organic aerosol (SOA) has been identified on the basis of thermal-resolved carbon fractions. Before the use of the thermal-resolved data, only eight instead of the final nine factors had been identified, and carbon content had been allocated to other factors by the PMF model. There is a noticeable difference between daytime and nighttime SOA factor contribution. In the summer, the average factor contribution at night was about 50% higher than that of daytime. In contrast, the average factor contribution at night in the winter was slightly lower than that of daytime.

The traffic primary factor profile is characterized by the highest percentage of nitrogen oxides of all the factors. It contains a group of elements typical for road traffic emissions, especially Cu, Zn, Ba, Fe, Mn, which originate from brake wear and from road resuspension. Although composition of the traffic markers can vary according the road type [17], significant percentages of these species in the factor profile clearly show the effect of brake, road, and tire wear. Apart from the above-mentioned species, EC and PAHs originating from exhaust emissions are present in the factor profile. Unlike the other chemical profiles, the only thermal-resolved fraction of significant contribution is EC3 here.

Relative contributions of the identified factors to the total PM_{2.5} mass are shown in Figure 5. As PM_{2.5} is the total variable, the results allow one to group this pollutant by monitoring sites. In contrast, for benzo[a]pyrene and arsenic, the total contributions have been modelled (See Figure 6).

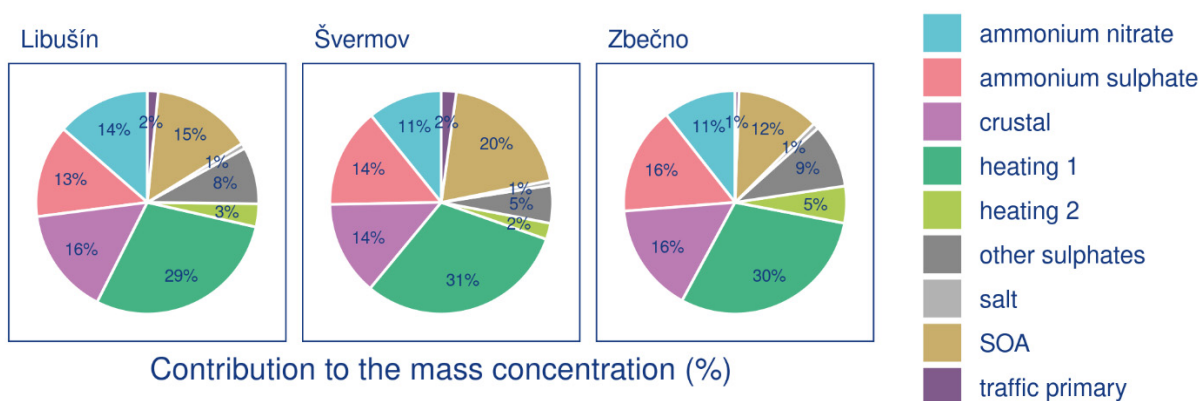


Figure 5. Relative factor contribution to the PM_{2.5} mass grouped by monitoring sites.

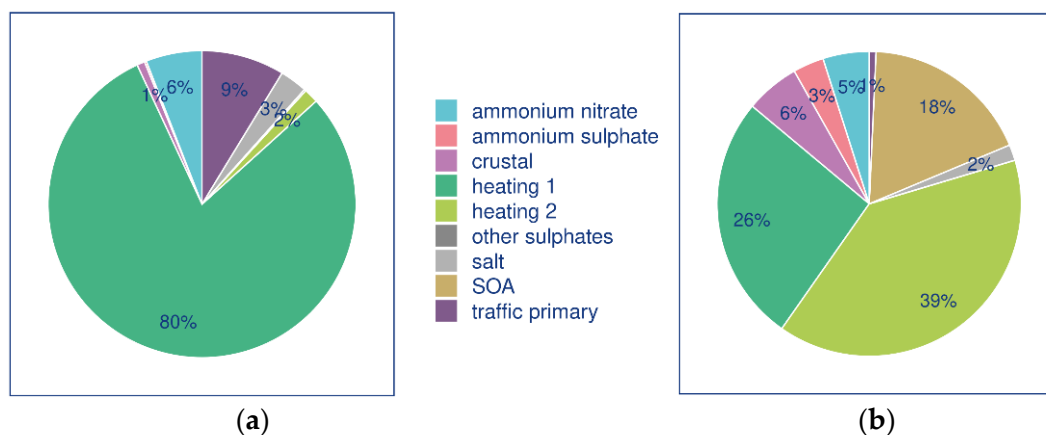


Figure 6. Overall relative factor contribution to benzo[a]pyrene (a) and arsenic (b) mass.

4. Discussion

4.1. Discussion of PMF Results Interpretation

Regarding the PM_{2.5} mass concentration, residential heating was the most important air pollution factor in the area of interest. Despite the fact that heating is of relevance only in the cold part of the year, it still represented the highest contribution to the annual PM_{2.5} concentration. The sum of the two identified heating factors accounts for approximately one third of the total PM_{2.5} concentrations. While the heating 1 factor had similar average contribution and variation at all the monitoring sites, there were significant differences in the case of the heating 2 factor. The contribution of the arsenic-rich heating 2 factor to PM_{2.5} concentrations was about two times higher in Zbečno than in Libušín and Švermov. The presence of arsenic and sulfur dioxide in the heating 2 factor chemical profile (see Appendix A) points to burning coal of low quality in Zbečno (with a high share of lignite, as it has high sulfur content [18] and high arsenic content of lignite mined in specific Czech regions [19]).

Similar to the residential heating factors, ammonium nitrate, ammonium sulfate, salt, and crustal factors' contributions can clearly be interpreted. Secondary ammonium nitrate and ammonium sulfate accounted in total for approximately one third of the PM_{2.5} mass at all the monitoring sites. They were thus important factors influencing air quality in those places. In the warm part of the year, ammonium sulfate had a far higher contribution to PM_{2.5} concentrations than ammonium nitrate, which was negligible. In the winter, the contribution of ammonium nitrate was higher than the contribution of ammonium sulfate.

The crustal factor had a significant contribution during the summer and low contribution during the winter. An exception is the situation at the monitoring site in Zbečno. There were several peak contributions here in the winter, probably due to the presence of a nearby all-year operating quarry (resuspension from the quarry area, from local roads used for stone transportation, and from the loading space of trucks). As opposed to the quarry impact in Zbečno, the crustal contribution in Libušín and Švermov is caused by resuspension from the paved city surfaces in the dry season. The crustal factor contribution was about 15% at all the monitoring sites.

As the salt factor had a significant relative contribution during both summer and winter, it can be assumed that the majority of it originated from sea aerosols. The slightly higher salt contribution in the winter can be attributed to road maintenance.

The sum of secondary inorganic aerosol factors (ammonium nitrate, ammonium sulfate, and other sulfates) had approximately as high a contribution to PM_{2.5} as the sum of both heating factors (heating 1 plus heating 2). For the necessary air pollution reduction in the area of interest, it is very important to mitigate both residential heating and secondary inorganic aerosol precursors emissions, e.g., from large combustion plants.

Further discussion is needed when interpreting the factors related to traffic. Based on the PMF model, primary traffic particles (exhaust emissions) account for only approxi-

mately one or two percent of the total $PM_{2.5}$ mass. The results show that far more significant air pollution in the area of interest is caused by secondary particles formation and road dust resuspension than by primary exhaust emissions. A road traffic emissions interference within the crustal PMF factor should be taken into account due to the similarity of both daily variation (higher contributions at daytime) and chemical composition (similar crustal particles are suspended by both vehicles from the road surface and by the wind from other surfaces). In addition, the relation between traffic emissions and the secondary organic aerosol (SOA) is shown in the PMF results. The time series of the factor contributions (see Appendix B) shows much higher contributions of SOA in Libušín and Švermov, which are strongly affected by traffic, unlike the rural monitoring site in Zbečno. A significant or even prevailing local origin of the SOA factor is indicated by the vigorous daily variation of its contribution (see Appendix B). An increased percentage of the higher-temperature carbon fractions (OC3, EC3—see Appendix A) in the SOA factor indicates a different source than residential heating (lower-temperature fractions in chemical profile are typical for local heating sources). The SOA, primary traffic and crustal are factors with a significant portion of higher-temperature carbon fractions. A small accessory amount of EC3 has also been assigned to the ammonium nitrate factor by the PMF model. SOA in Libušín and Švermov thus seems to be induced largely by the local road traffic, especially in the winter, when the factor contribution difference between Zbečno and the other two sites is significant. Based on the facts mentioned above, the total traffic contribution to the $PM_{2.5}$ mass should be estimated not only from the contribution of the traffic primary factor, but also from part of the SOA, crustal, and ammonium nitrate factors. The winter contribution of the SOA factor was about two times higher at Libušín and about three times higher in Švermov (the most traffic-influenced site) than at the rural site of Zbečno. Therefore, it can be assumed that the traffic-induced amount of SOA was negligible in Zbečno, and about half and two thirds of SOA contribution originated from traffic emissions in Libušín and Švermov, respectively. On the basis of the comparison between the different monitoring sites, it can be assumed that in the summer, there was a non-negligible traffic contribution to the crustal factor due to road resuspension. Libušín and Švermov had at least about a 25% higher contribution to the crustal factor in the summer (see Figure 4), despite the presence of the quarry in Zbečno, which is a potential significant contributor to this factor. In the winter, there was a higher contribution to the crustal factor in Zbečno than at the other sites, probably due to very limited resuspension from wet or frozen road surfaces (fugitive dust from the local quarry was the only significant contribution to the crustal factor in the winter). It is very difficult to estimate the local traffic contribution to the ammonium nitrate factor. As mentioned above and in other studies, e.g., [20], there are indicators that the influence of traffic emissions on the ammonium nitrate formation is significant, but further information needed for the quantification of such an effect is missing. Because of the above-mentioned reasons, the total impact of local traffic on air quality could not be directly quantified by the PMF model. Based on the above information, one can estimate the total relative contribution of local traffic to the $PM_{2.5}$ mass concentration (sum of the traffic primary factor and the estimation of the traffic contribution to the crustal and the SOA factors) as follows: up to 5% in Zbečno, about 15–20% in Libušín, and about 20–25% in Švermov. These values represent only the local traffic contribution at the monitoring sites. The contribution of regional traffic, which is probably part of the identified ammonium nitrate and the “SOA” factors, is impossible to quantify and was thus not calculated.

The other sulfates” PMF factor was hard to explain without further analysis. Therefore, hourly back trajectories covering the whole sampling period were batch-processed. Back trajectories based on the hourly meteorological data were used, while the aerosol sampling was made with a sampling duration of 12 h. Therefore, 12 trajectories were assigned to each of the samples. The contribution of the other sulfates factor to the $PM_{2.5}$ concentration was then assigned to each of such 12 back trajectories. Subsequently, all the trajectories with the assigned factor contribution were converted to raster layers and overlaid in GRASS GIS. (For overlapping trajectories, the factor contributions assigned to the individual trajectories were averaged

out.) Trajectories with a high factor contribution to $PM_{2.5}$ were visually accentuated by the nearest neighbor method using a 90th percentile in the moving window. The analysis result is shown in Figure 7. Violet points in Figure 7 represent positions of large combustion plants (LCPs) with sulfur oxides emissions exceeding 100 tons per year. The analysis is based on The European Pollutant Release and Transfer Register (E-PRTR) data of the year 2019 [21]. Unfortunately, information about locations and emissions of German LCPs were not published in The European Pollutant Release and Transfer Register, so they are not shown in Figure 7. Nevertheless, the graphical analysis result indicates that a significant part of the other sulfates factor contribution to $PM_{2.5}$ is related to LCPs operation. (See red-marked areas in Figure 7).

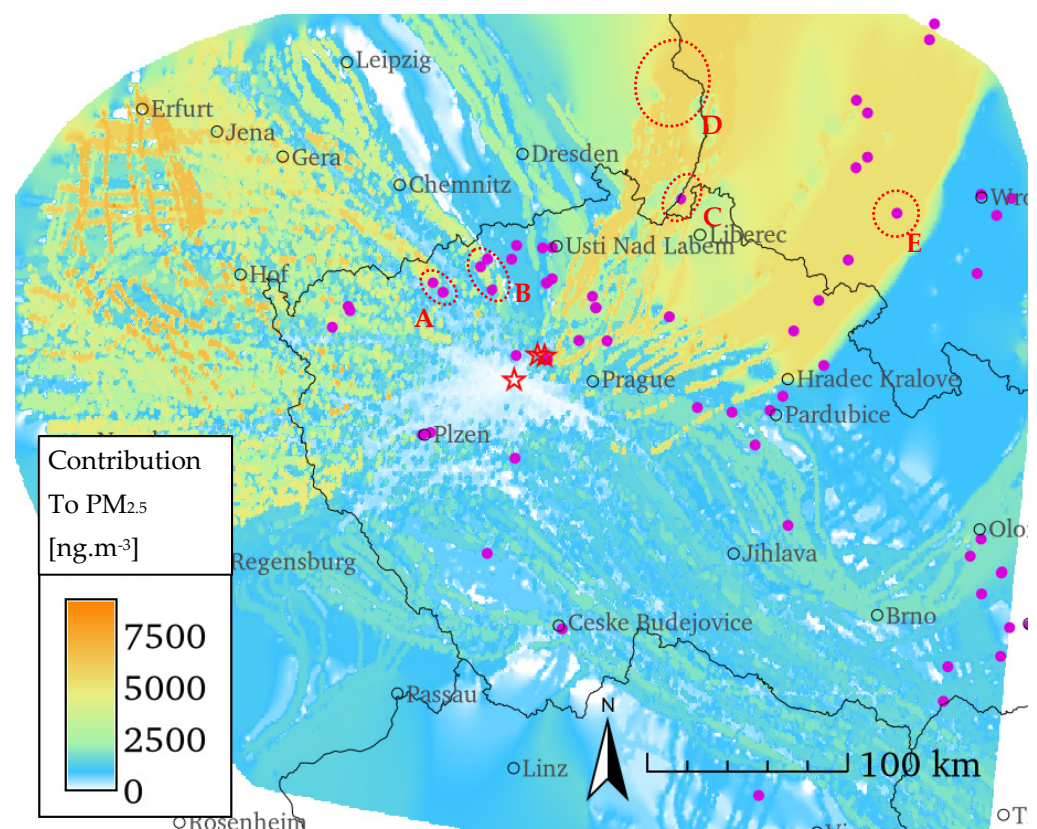


Figure 7. Visualization of batch-processed back trajectories for the other sulfates factor. Dashed red lines delimit potential sources: A—Pruněřov and Tušimice power plants; B—Počerady and Komořany power plants and Unipetrol RPA chemical installation; C—Turów power plant; D—Jänschwalde, Boxberg, and Schwarze Pumpe power plants; E—Polski Koncern Naftowy ORLEN S.A. oil refinery.

The distance to the German lignite-burning power plants located in the area marked as “D” (surroundings of the Cottbus city) is longer than to the Czech sources from the area of interest, but installed power in the eastern Germany is considerably higher. For Jänschwalde, Boxberg, and Schwarze Pumpe power plants, it is 3, 2.575 and 1.6 GWe, respectively [22]. The total installed power of the lignite burning LCPs here is the second highest in Germany [23]. The maximum installed power of the individual power plants in the Czech part of Figure 7 is only 0.66 GW (Tušimice and Pruněřov). Emissions of sulfur and nitrogen oxides from the German installations have thus possibly a significant impact on secondary aerosol formation. Similarly, the Polish source “E” with 4.65 kt SO_2 emissions per year is potentially a far more important sulfates precursors source than other Czech and Polish sources shown in Figure 7. (The maximum annual SO_2 emission of the other Czech and Polish sources is one order of magnitude lower [21].) Additionally, species composition (soluble ions including sulfates, vanadium, and selenium) of the other sulfates factor

points to emissions from non-local sources, probably coal-burning large combustion plants. A lower factor contribution in the winter compared with the summer may be related to different conditions for secondary aerosol formation. Individual species contribution can be partly included in the ammonium sulfate or the ammonium nitrate factor in the winter. Based on the above information, the other sulfates factor was probably predominantly composed from secondary particles induced by the emissions from large industrial power plants and oil refinery installations.

As both benzo[*a*]pyrene and arsenic are predominantly related to residential heating (see Figure 6), it is clear that the main air pollution problems in the area of interest are caused especially by the local heating sources.

About 80% of benzo[*a*]pyrene comes from residential heating. The second most important contributor is road traffic (primary exhaust particles) in the area of interest (average contribution of about 10%). Regarding the traffic contribution to the benzo[*a*]pyrene concentration, large spatial differences in traffic load among the sites cannot be neglected. In Švermov and Libušín, it is relevant to assume that traffic contribution to benzo[*a*]pyrene concentrations is at or slightly over 10%, while at rural sites, e.g., in Zbečno, it is nearly zero.

The arsenic contribution from residential heating is strongly site-specific in the area of interest. Locally and temporarily, it can be very high, due to the use of specific coal fuel (probably with a higher ratio of lignite). The arsenic contribution linked to the heating 2 factor was predominantly caused by several peak concentrations during the winter part of the monitoring period (only one month of measurement). Additionally, most of arsenic mass in the heating 2 factor profile originated from only one of the monitoring sites (Zbečno). These two reasons led to the limited number of samples with high arsenic concentrations in the model dataset compared to time distribution of high concentrations of PM_{2.5} and benzo[*a*]pyrene. The multilinear engine within the PMF model was thus not able to fit the predicted arsenic concentration to the measured values as closely as in the case of PM_{2.5} and benzo[*a*]pyrene. These are the reasons why the correlation between the observed and predicted arsenic concentrations (R^2) is significantly lower than in the case of PM_{2.5} and benzo[*a*]pyrene.

A strong impact of residential heating on the PM_{2.5}, benzo[*a*]pyrene, and arsenic concentrations is also apparent from the following molecular markers concentration evaluation, which was done independently of the PMF model.

4.2. Discussion on Organic Molecular Markers Concentrations

For the purposes of this study, some markers were selected, which have been proved to be suitable organic molecular tracers for the identification of the main anthropogenic sources of particulate matter, such as the combustion of fossil fuels, biomass burning, including wood and grass, and vehicular emissions. The concentrations of fifteen PAHs, six hopanes, six steranes, and three anhydrosugars in the PM_{2.5} aerosol samples were measured.

Polycyclic aromatic hydrocarbons (PAHs) are a group of organic substances that is receiving particular attention because some PAHs are considered to be carcinogens and mutagens [24]. PAHs are mostly formed from the incomplete combustion of a variety of fuels emitted by different source types, including household heating, industrial processes, waste incineration, and mobile sources [25,26]. Benzo[*a*]pyrene is the only PAH that has a legislative limit (1 ng·m⁻³ annual average concentration), and it was used as a marker for carcinogenic risk assessment [27]. All measured PAH concentrations show a large seasonal variation between summer and winter campaigns, spanning more than one order of magnitude from winter maximum to summer minimum values. Across all three sites, the BaP concentrations were two orders of magnitude higher for the winter samples (average of 3.83 ng·m⁻³) than for the summer samples (average of 0.03 ng·m⁻³). The seasonal differences can be explained by a decreased residential heating intensity during warm months and increased photolysis and dispersion of all PAHs. Very low summer concentrations are due to the lack of large industrial sources of pollution in the vicinity and due to larger distance from major roads. The rest of the measured PAH concentrations

showed less significant seasonal differences than BaP with the exception of BaA (winter concentrations were between 140 and 330 times higher), which is highly susceptible to photo-oxidation [25,28]. Picene was selected as a marker for the coal combustion. Retene was used as one of the markers of burning coniferous wood. During the summer, their concentrations were below the detection limit of the method, with the exception of four night samples from Zbečno. During the winter, both markers, retene and picene, were present in all samples. The PAH's detection limits were $0.03 \text{ ng}\cdot\text{m}^{-3}$ except those of picene and coronene ($0.04 \text{ ng}\cdot\text{m}^{-3}$), pyrene and retene ($0.06 \text{ ng}\cdot\text{m}^{-3}$), and fluoranthene ($0.08 \text{ ng}\cdot\text{m}^{-3}$).

The change in PAH profiles detected during the summer and winter seasons showed a need to investigate the nature of the PAHs emissions by analyzing the diagnostic ratios of the individual congeners concentrations. The following PAH diagnostic ratios were investigated: BeP/(BeP + BaP), BaP/BghiPRL, BaA/(BaA + CRY), RET/(RET + CRY), and I123cdP/(I123cdP + BghiPRL). In this study, only two diagnostic ratios that showed large seasonal variations and have a good explanatory power/ability to distinguish sources of emissions are described. The first diagnostic ratio selected is the BeP/(BeP + BaP), which can be used as an indicator of the aging of aerosol particles [29,30]. During the summer, the ratio BeP/(BeP + BaP) at all three sampling sites was in the range from 0.4 to 0.7, indicating regional or long-distance transport of aerosols. In contrast, in the winter, this ratio was less than 0.5 (in the range from 0.29 to 0.54, average of 0.39), which indicates major emissions of aerosols from local sources. During the winter, the values of the BeP/(BeP + BaP) ratio corresponds to the combustion of coal and wood. According to the literature, typical values for the combustion of brown and black coal in various boilers are in the range of 0.28 to 0.42 [31] and for wood burning around 0.34 [29].

Another selected diagnostic ratio that shows a large seasonal variation is BaP/BghiPRL. During the winter, the values of BaP/BghiPRL range between 0.76 and 1.8 (average of 1.24) and summer values decrease to 0.35, but the average value is 0.68. Various authors report values in the range of 0.3 to 0.4 for gasoline cars, while values in the range of 0.4 to 0.8 for diesel cars, wood combustion emissions are estimated in the range of 1.5 to 2, and values larger than 1.20 are proposed for coal combustion in house heating [29,32,33]. During the winter, the values of the BaP/BghiPRL ratio correspond to those mentioned in literature, which are typical for combustion of coal and wood, while in the summer they correspond to the values typical for traffic emissions.

The next two groups of markers analyzed are hopanes and steranes. These are considered to be markers for traffic emissions in the atmosphere [34,35]. Both groups of compounds are present in lubricating oil used by both gasoline- and diesel-powered motor vehicles but are not present in the fuels as such. On the other hand, only hopanes are present in emissions from coal combustion, and their diagnostic ratios are used to identify the combustion of different coal types [36]. For example, the characteristic ratio between concentrations of 22R-17 α (H),21 β (H)-homohopane and 22S-17 α (H),21 β (H)-homohopane, known as the homohopane index, is in the range of 0.05 to 0.40 and increases with the maturity of the coal—0.05 for lignite, 0.08 for brown coal, 0.20 for sub-bituminous coal, and 0.37 for bituminous coal [36]. According to the literature, the homohopane index C31 α β [S/(S + R)] for traffic emissions ranges from 0.45 to 0.60 [35,37].

Across all three sites, the steranes concentrations were very low or below the detection limit ($0.04 \text{ ng}\cdot\text{m}^{-3}$) in samples from both summer and winter campaigns. The most abundant sterane in the summer samples was $\alpha\alpha\alpha$ 20R-Cholestane (average $0.06 \text{ ng}\cdot\text{m}^{-3}$), and its concentrations in the winter samples remain at the same level (average of $0.05 \text{ ng}\cdot\text{m}^{-3}$). Steranes do not show seasonal variation, and their low concentrations indicate the negligible impact of mobile sources. In contrast, hopanes show large seasonal differences. During the summer, hopanes concentrations at all three locations were very low or below the detection limits, and homohopane indexes were in the range from 0.37 to 0.57 (average of 0.51), which indicates that hopanes in the summer samples originated mainly from traffic emissions. During the winter campaign, hopanes concentrations across all the three sites were on average one order of magnitude higher than in the case of the summer sam-

ples. The calculated mean value of the homohopane index was 0.15, which indicates that hopanes in the winter samples originated mainly from low-rank coal combustion. Because of very low calculated homohopane indexes for some of the samples, one can assume combustion of more lignite coal during the winter season in Zbečno. Monosaccharide anhydrides are commonly used as tracers for the combustion of biomass, which contains cellulose, hemicellulose, and lignin. Analysis of levoglucosan (L), mannosan (M) and galactosan (G) simultaneously in each sample can be of major benefit due to the fact that their ratios (L/M, L/G, L/M + G) can help to distinguish the type of biomass burned. The explanatory power of these ratios is similar; therefore, only the L/M ratio was used. The L/M ratio varies significantly for different types of wood burned. Various authors report values in the range of 2.5 to 6.7 for burning softwood [38–40], while values in the range of 13 to 24 are typical for hardwood [38,40]. Values are in the range of 2 to 33, with an average of 23 [41], are typical for grasses. Recent research suggests that levoglucosan is not released exclusively during biomass combustion but is also present in emissions from some types of lignite. Therefore, the burning of lignite can mean an additional input of levoglucosan into the atmosphere in regions where low-rank coal is utilized as a domestic fuel [42]. Fortunately, anhydrosaccharides ratios in lignite smoke differ from those from biomass burning and the L/M ratio for lignite is in the range of 31 to 92 [41].

Across all three sites, levoglucosan concentrations were between 20 and 35 times higher in the winter samples (average of $814.6 \text{ ng}\cdot\text{m}^{-3}$) than in the summer samples (average of $31.9 \text{ ng}\cdot\text{m}^{-3}$). The seasonal differences can be attributed to a decreased extent of wood burning for residential heating during the warm months. In contrast, the L/M ratio, which indicates the type of biomass burned, did not show seasonal differences, with the exception of the Zbečno sampling site. During the summer, L/M ratios for the Kladno, Libušín, and Zbečno sampling sites were 4.14, 6.42 and 5.55, respectively, which indicates primarily burning softwood. During the winter, L/M ratios for Kladno and Libušín remained at the same level, 5.70 and 6.46, respectively, which shows that there is no change in the dominant type of wood being burned. For the sampling site of Zbečno, the calculated L/M ratios were more variable than at the other two sites and were in the range of 1.99 to 88.5 (average of 11.2). The average value for the L/M ratio during the winter campaign was twice as high as during the summer, but this does not mean that a different type of wood was burned because the median remained at the same value of 4.37. There were several high values of the L/M ratio in the range between 49.5 and 88.5, which, according to the literature, indicate the combustion of lignite. This fact confirms the suspicion based on low values of the homohopane index calculated for this sampling site that lignite was used for household heating in Zbečno.

Analysis of seasonal variation of the selected organic markers supports the simultaneous contribution from different sources, with major influence of residential heating during the winter and traffic-related sources during the summer (see Figure 8).

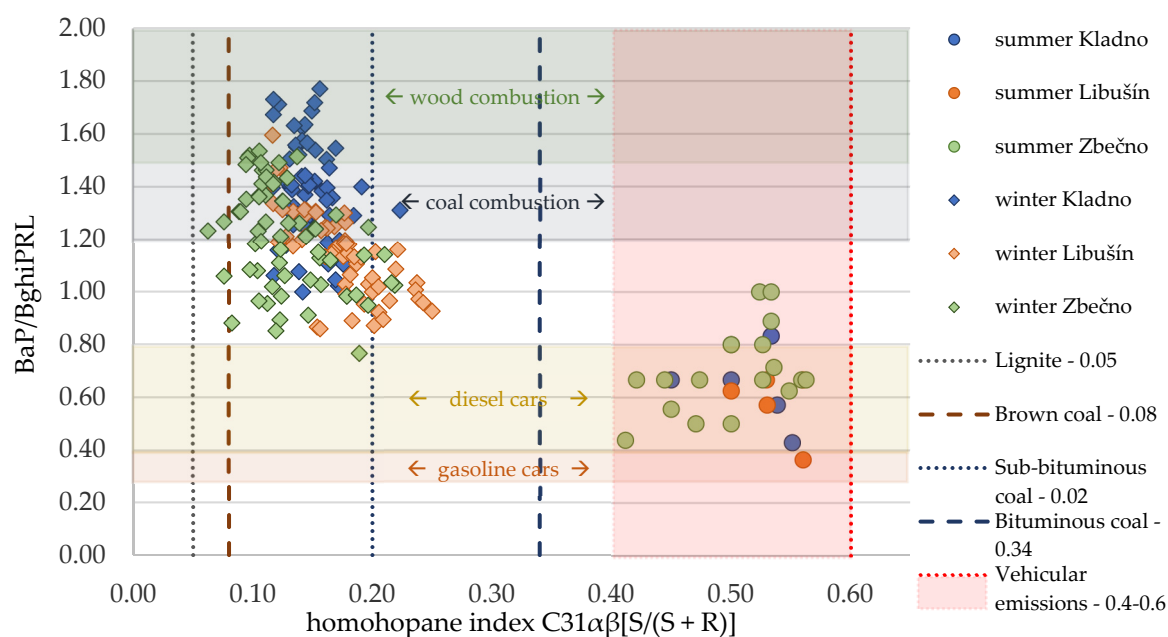


Figure 8. Cross plot for the ratio of BaP/BghiPRL to homohopane index $C_{31}\alpha\beta[S/(S + R)]$. The different symbols and colors identify measurements performed during the winter (diamonds) and summer (circles) at the three sampling sites (blue—Švermov, orange—Libušín, green—Zbečno).

5. Conclusions

The measurements performed at the three sites for the purpose of the PMF model verified the previous air monitoring results [1,10,11], which pointed out increased concentrations of $PM_{2.5}$, benzo[*a*]pyrene, and arsenic in the area of interest. The PMF results clearly showed that the main problem of air quality in this area is individual residential heating by solid fuels. Primary particles emitted from these installations represent about one third of the total $PM_{2.5}$ mass concentration. Residential heating was the most important source of primary $PM_{2.5}$ in the area of interest. Moreover, the PMF results indicate that residential heating emissions play an important role in the SOA formation in these places. The total impact of residential heating on air pollution was thus even more significant than just the aforementioned contribution of primary particles.

The quantification of traffic sources contribution to $PM_{2.5}$ was quite challenging due to the fact that the effect of road traffic is manifested within multiple PMF factors (primary traffic particles, SOA, ammonium nitrate). An estimation of the total traffic contribution to $PM_{2.5}$ significantly differs among the monitoring sites. It is about 5% in Zbečno, 15–20% in Libušín, and 20–25% in Švermov. The road traffic contribution in Švermov and Libušín is thus the second highest from the local anthropogenic sources affecting air quality at these sites.

Regarding the contribution of local sources to $PM_{2.5}$, the third most important were mineral dust particles (non-road resuspended dust and emissions from mineral resources exploitation). Their contribution to $PM_{2.5}$ was about 15% at all the monitoring sites. The contribution of aged sea salt was insignificant (only about 1% of $PM_{2.5}$).

A large portion of $PM_{2.5}$ mass consisted of various secondary aerosol particles (ammonium nitrate, ammonium sulfate, other sulfates, and SOA) which accounted for approximately 50% of $PM_{2.5}$ at all three monitoring sites. A significant proportion of SOA (contribution to $PM_{2.5}$ between 10 and 20%, depending on the particular monitoring site) and ammonium nitrate (contribution from 10 to 15%) is assumed to be of local or near-regional origin (effect of both road traffic and residential heating emissions).

On the other hand, the other sulfates (approximately 5–10% of $PM_{2.5}$) and ammonium sulfate (about 15% of $PM_{2.5}$) factors originated from distant sources (from 50 to thousands of kilometers). Their contribution is thus not possible to decrease by potential future local

air quality measures. The contribution of the other sulfates and the ammonium sulfate factors is associated with large combustion plants operation (noticeable especially in the summer, when emissions from seasonally operating heating sources are negligible) and with residential heating (part of the contribution of the “ammonium sulfate” factor in the winter).

In order to decrease the PM_{2.5} concentrations in the area of interest, the highest priority is nowadays to reduce local emissions originating from residential heating. Despite the major role of residential heating, research results show that the continuation of mitigating measures focused on industrial power generation in the Czech Republic and surrounding countries is needed for effective air protection in the area of interest. Regarding the PM_{2.5}, mitigating traffic emissions would be less significant in these places due to the low or only moderate traffic intensity.

The increased arsenic concentrations and their significant local variation among the monitoring sites was caused predominantly by the burning of lignite or other arsenic-rich coal in households. Relatively high benzo[*a*]pyrene concentrations at the monitoring sites were caused by residential heating in the area of interest (both coal and biomass burning). The PMF results regarding arsenic and PAH pollution sources are in line with the conclusions of the independently performed evaluation of molecular markers concentrations.

Potential measures focused on residential heating are very important for mitigating all of the main air quality problems in the area of interest (increased PM_{2.5}, arsenic, and benzo[*a*]pyrene concentrations). Due to the positive leverage effect, decreasing emissions from burning coal and biomass in households is thus strongly preferred in the area of interest.

Supplementary Materials: The following are available online at <https://www.mdpi.com/article/10.3390/environments8100107/s1>, Table S1: Measured concentrations and uncertainties.

Author Contributions: Conceptualization: V.V., B.K. and D.H.; methodology: V.V., B.K., D.H. and R.S.; formal analysis: R.S., I.N. and V.V.; investigation: R.S. and I.N.; resources: R.S., I.N. and D.H.; data curation: R.S. and D.H.; writing—original draft preparation: R.S.; writing—review and editing: Jáchym Brzezina, I.N., V.V. and B.K.; visualization: R.S.; supervision: B.K.; project administration: R.S. All authors have read and agreed to the published version of the manuscript.

Funding: This research was funded by the Technology Agency of the Czech Republic, grant number TITSMZP704.

Data Availability Statement: Data is contained within the supplementary material.

Conflicts of Interest: The authors declare no conflict of interest. The funders had no role in the design of the study; in the collection, analyses, or interpretation of data; in writing the manuscript; or in the decision to publish the results.

Appendix A

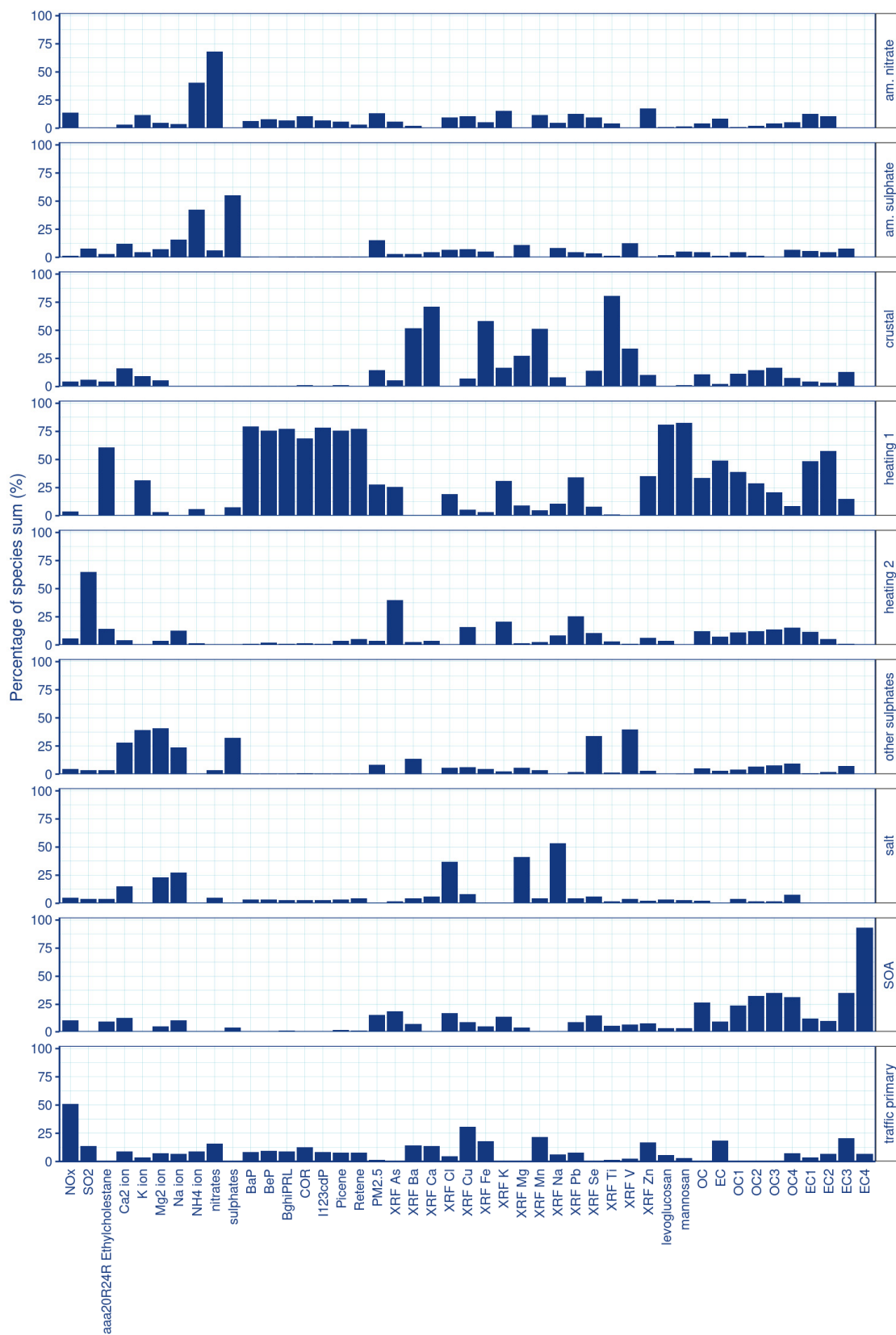


Figure A1. Percentage of species sum in factor profiles.

Appendix B



Figure A2. Factor contributions to the PM_{2.5} mass concentration.

References

1. CHMI. *Air Pollution in the Czech Republic in 2019*, 1st ed.; Czech Hydrometeorological Institute: Prague, Czech Republic, 2020; ISBN 9788076530133. Available online: https://www.chmi.cz/files/portal/docs/uoco/isko/grafroc/19groc/gr19en/19_rocenka_uko_EN_v3.pdf (accessed on 25 May 2021).
2. CHMI. Air Pollution and Atmospheric Deposition in Data, the Czech Republic, 2016. Summary Tabular Survey. 2017. Available online: https://www.chmi.cz/files/portal/docs/uoco/isko/tab_roc/2016_enh/index_GB.html (accessed on 25 May 2021).
3. CHMI. Air Pollution and Atmospheric Deposition in Data, the Czech Republic, 2017. Summary Tabular Survey. 2018. Available online: https://www.chmi.cz/files/portal/docs/uoco/isko/tab_roc/2017_enh/index_GB.html (accessed on 25 May 2021).
4. CHMI. Air Pollution and Atmospheric Deposition in Data, the Czech Republic, 2018. Summary Tabular Survey. 2019. Available online: https://www.chmi.cz/files/portal/docs/uoco/isko/tab_roc/2018_enh/index_GB.html (accessed on 25 May 2021).
5. CHMI. Air Pollution and Atmospheric Deposition in Data, the Czech Republic, 2019. Summary Tabular Survey. 2020. Available online: https://www.chmi.cz/files/portal/docs/uoco/isko/tab_roc/2019_enh/index_GB.html (accessed on 25 May 2021).
6. Zákon, Č. 201/2012 Sb. ze dne 2. Května 2012 o Ochráně Ovzduší (Act No. 201/2012 Coll. of 2 May 2012 on Air Protection); Tiskárna Ministerstva vnitra: Praha, Czech Republic, 2012; pp. 2785–2848. (In Czech)
7. CHMI. *Air Pollution in the Czech Republic in 2016*, 1st ed.; Czech Hydrometeorological Institute: Prague, Czech Republic, 2017; ISBN 9788087577721. Available online: https://www.chmi.cz/files/portal/docs/uoco/isko/grafroc/16groc/gr16en/KO_rocenka_2016.pdf (accessed on 25 May 2021).
8. TAČR (Technology Agency of the Czech Republic). Analysis of PAH and Selected Organic Markers from Ambient Air in Small Municipalities. Project from Programme BETA 2 Is Realized in Years 2018–2021 (Measurement and Analysis of Air Pollution with Emphasis on Evaluating the Share of Individual Groups of Sources. TITSMZP704). 2018. Available online: https://starfos.tacr.cz/en/result/RIV%2F00020699%3A_____%2F19%3AN0000194 (accessed on 11 October 2021).
9. TAČR (Technology Agency of the Czech Republic). Evaluation of the Effectiveness of Air Quality Improvement Programs in Small Settlements—Winter 2017/2018—Summary Report on Measurement Results and Basic Evaluation of Results. Project from Programme BETA2 Is Realized in Years 2018–2021 (Measurement and Analysis of Air Pollution with Emphasis on Evaluating the Share of Individual Groups of Sources. TITSMZP704). 2018. Available online: https://starfos.tacr.cz/cs/result/RIV%2F00020699%3A_____%2F18%3AN0000184 (accessed on 11 October 2021).
10. CHMI. *Air Pollution in the Czech Republic in 2017*, 1st ed.; Czech Hydrometeorological Institute: Prague, Czech Republic, 2018; ISBN 9788087577837. Available online: https://www.chmi.cz/files/portal/docs/uoco/isko/grafroc/17groc/gr17en/KO_rocenka_2017.pdf (accessed on 25 May 2021).
11. CHMI. *Air Pollution in the Czech Republic in 2018*, 1st ed.; Czech Hydrometeorological Institute: Prague, Czech Republic, 2019; ISBN 9788087577950. Available online: https://www.chmi.cz/files/portal/docs/uoco/isko/grafroc/18groc/gr18en/KO_rocenka_2018.pdf (accessed on 25 May 2021).
12. TAČR (Technology Agency of the Czech Republic). Measurement and Analysis of Air Pollution with Emphasis on Evaluating the Share of Individual Groups of Sources. TITSMZP704, Project from Programme BETA 2 Is Realized in Years 2018–2021. 2018. Available online: <https://starfos.tacr.cz/en/project/TITSMZP704#project-main> (accessed on 11 October 2021).
13. Road and Motorway Directorate of the Czech Republic. National Traffic Census. 2016. Available online: <http://scitani2016.rsd.cz/pages/informations/default.aspx> (accessed on 9 August 2021).
14. Contini, D.; Cesari, D.; Conte, M.; Donato, A. Application of PMF and CMB receptor models for the evaluation of the contribution of a large coal-fired power plant to PM₁₀ concentrations. *Sci. Total Environ.* **2016**, *560*, 131–140. [CrossRef]
15. Norris, G.; Duvall, R.; Brown, S.; Bai, S. *Positive Matrix Factorization (PMF), Fundamentals and User Guide*; U. S. EPA: Washington, DC, USA, 2014. Available online: https://www.epa.gov/sites/production/files/2015-02/documents/pmf_5.0_user_guide.pdf (accessed on 9 August 2021).
16. Lebrato, M.; Garbe-Schönberg, D.; Müller, M.N.; Blanco-Ameijeiras, S.; Feely, R.A.; Lorenzoni, L.; Molinero, J.-C.; Bremer, K.; Jones, D.O.B.; Iglesias-Rodríguez, D.; et al. Global variability in seawater Mg:Ca and Sr:Ca ratios in the modern ocean. *Proc. Natl. Acad. Sci. USA* **2020**, *117*, 22281. [CrossRef]
17. Amato, F.; Alastuey, A.; de la Rosa, J.; Gonzalez Castanedo, Y.; Sánchez de la Campa, A.M.; Pandolfi, M.; Lozano, A.; Contreras González, J.; Querol, X. Trends of road dust emissions contributions on ambient air particulate levels at rural, urban and industrial sites in southern Spain. *Atmos. Chem. Phys.* **2014**, *14*, 3533–3544. [CrossRef]
18. Bouška, V.; Pešek, J. Quality parameters of lignite of the North Bohemian Basin in the Czech Republic in comparison with the world average lignite. *Int. J. Coal Geol.* **1999**, *40*, 211–235. [CrossRef]
19. Pešek, J.; Bencko, V.; Sýkorová, I.; Vašíček, M.; Michna, O.; Martínek, K. Some trace elements in coal of the Czech Republic, Environment and health protection implications. *Cent. Eur. J. Public Health* **2005**, *2005*, 153–158.
20. Ehrnsperger, L.; Klemm, O. Source Apportionment of Urban Ammonia and its Contribution to Secondary Particle Formation in a Mid-size European City. *Aerosol Air Qual. Res.* **2021**, *21*, 200404. [CrossRef]
21. The European Pollutant Release and Transfer Register (E-PRTR). Available online: <https://www.eea.europa.eu/data-and-maps/data/industrial-reporting-under-the-industrial-3> (accessed on 10 August 2021).
22. EP Power Europe (EPPE). Available online: <https://www.eppowereurope.cz/en/business-areas/prehled-segmentu/> (accessed on 10 August 2021).

23. Germany Looks to Step Up Coal Exit Timetable. Available online: <https://ednh.news/germany-looks-to-step-up-coal-exit-timetable/> (accessed on 10 August 2021).
24. IARC. Vol 105: Diesel and gasoline engine exhaust and some nitroarenes. In *IARC Monographs on the Evaluation of Carcinogenic Risks to Humans*; International Agency for Research on Cancer: Lyon, France, 2013; Volume 105.
25. Ravindra, K.; Sokhi, R.; Van Grieken, R. Atmospheric polycyclic aromatic hydrocarbons: Source attribution, emission factors and regulation. *Atmos. Environ.* **2008**, *42*, 2895–2921. [[CrossRef](#)]
26. Dyke, P.H.; Foan, C.; Fiedler, H. PCB and PAH releases from power stations and waste incineration processes in the UK. *Chemosphere* **2003**, *50*, 469–480. [[CrossRef](#)]
27. Directive 2004/107/EC of the European Parliament and of the Council. Available online: <https://eur-lex.europa.eu/legal-content/EN/TXT/?uri=CELEX:32004L0107> (accessed on 11 October 2021).
28. Schauer, C.; Niessner, R.; Poschl, U. Polycyclic aromatic hydrocarbons in urban air particulate matter: Decadal and seasonal trends, chemical degradation, and sampling artifacts. *Environ. Sci. Technol.* **2003**, *37*, 2861–2868. [[CrossRef](#)]
29. Alves, C.A. Characterisation of solvent extractable organic constituents in atmospheric particulate matter: An overview. *An. Acad. Bras. Cienc.* **2008**, *80*, 21–82. [[CrossRef](#)]
30. Oliveira, C.; Martins, N.; Tavares, J.; Pio, C.; Cerqueira, M.; Matos, M.; Silva, H.; Oliveira, C.; Camões, F. Size distribution of polycyclic aromatic hydrocarbons in a roadway tunnel in Lisbon, Portugal. *Chemosphere* **2011**, *83*, 1588–1596. [[CrossRef](#)]
31. Krůmal, K.; Mikuška, P.; Horák, J.; Hopan, F.; Kubaňová, L. Influence of boiler output and type on gaseous and particulate emissions from the combustion of coal for residential heating. *Chemosphere* **2021**, *278*, 130402. [[CrossRef](#)] [[PubMed](#)]
32. Cecinato, A.; Guerriero, E.; Balducci, C.; Muto, V. Use of the PAH fingerprints for identifying pollution sources. *Urban Clim.* **2014**, *10*, 630–633. [[CrossRef](#)]
33. Finardi, S.; Radice, P.; Cecinato, A.; Gariazzo, C.; Gherardi, M.; Romagnoli, P. Seasonal variation of PAHs concentration and source attribution through diagnostic ratios analysis. *Urban Clim.* **2017**, *22*, 19–34. [[CrossRef](#)]
34. Simoneit, B.R.T. A review of biomarker compounds as source indicators and tracers for air pollution. *Environ. Sci. Pollut. Res.* **1999**, *6*, 159–169. [[CrossRef](#)]
35. Schauer, J.J.; Rogge, W.F.; Hildemann, L.M.; Mazurek, M.A.; Cass, G.R.; Simoneit, B.R.T. Source apportionment of airborne particulate matter using organic compounds as tracers. *Atmos. Environ.* **1996**, *30*, 3837–3855. [[CrossRef](#)]
36. Oros, D.R.; Simoneit, B.R.T. Identification and emission rates of molecular tracers in coal smoke particulate matter. *Fuel* **2000**, *79*, 515–536. [[CrossRef](#)]
37. Rogge, W.F.; Hildemann, L.M.; Mazurek, M.; Cass, G.R.; Simoneit, B.R.T. Sources of fine organic aerosol: 2. Noncatalyst and catalyst-equipped automobiles and heavy-duty diesel trucks. *Environ. Sci. Technol.* **1993**, *27*, 636–651. [[CrossRef](#)]
38. Fine, P.M.; Cass, G.R.; Simoneit, B.R.T. Chemical characterization of fine particle emissions from fireplace combustion of woods grown in the midwestern and western United States. *Environ. Eng. Sci.* **2004**, *21*, 387–409. [[CrossRef](#)]
39. Engling, G.; Carrico, C.M.; Kreidenweis, S.M.; Collett, J.L., Jr.; Day, D.E.; Malm, W.C.; Lincoln, W.C.; Hao, W.M.; Iinuma, Y.; Herrmann, H. Determination of levoglucosan in biomass combustion aerosol by high-performance anionexchange chromatography with pulsed amperometric detection. *Atmos. Environ.* **2016**, *40*, 299–311. [[CrossRef](#)]
40. Schmidl, C.; Marr, I.L.; Caseiro, A.; Kotianová, P.; Berner, A.; Bauer, H.; Kasper-Giebl, A.; Puxbaum, H. Chemical characterisation of fine particle emissions from wood stove combustion of common woods growing in mid-European Alpine regions. *Atmos. Environ.* **2018**, *42*, 126–141. [[CrossRef](#)]
41. Oros, D.R.; Radzi bin Abas, M.; Omar, N.Y.M.J.; Rahman, N.A.; Simoneit, B.R.T. Identification and emission factors of molecular tracers in organic aerosols from biomass burning: 3. Grasses. *Appl. Geochem.* **2006**, *21*, 919–940. [[CrossRef](#)]
42. Fabbri, D.; Torri, C.; Simoneit, B.R.T.; Marynowski, L.; Rushdi, A.I.; Fabiańska, M.J. Levoglucosan and other cellulose and lignin markers in emissions from burning of Miocene lignites. *Atmos. Environ.* **2009**, *43*, 2286–2295. [[CrossRef](#)]